# Cytoarchitecture of cortex imaged by Optical Coherence Tomography

Caroline Magnain, Jean Augustinack, Martin Reuter, Bruce Fischl and David Boas

Athinoula A. Martinos Center for Biomedical Imaging, Department of Radiology, Massachusetts General Hospital/Harvard Medical School, Charlestown, Massachusetts, 02129, USA

MGH/HST Athinoula A. Martinos Center for Biomedical Imaging

MASSACHUSETTS GENERAL HOSPITAL

Harvard-MIT Health Sciences & Technology

## Introduction

Brodmann areas (BA) differ from one another in cytoarchitecture [3]. While brain mapping has improved with *ex vivo* MRI and histological validation, the resolution of MRI has limits that constrain our ability to visualize these features, even *ex vivo*. Moreover, refined localization of brain areas is critical for brain mapping as well as application to cortical diseases such as Alzheimer's disease. Although *in vivo* biomarkers exist, many definitive diagnoses still rest on autopsy evaluation of histological tissue. Histology is labor intensive and prone to irremediable distortions due to cutting, mounting and staining, which render registration across slices and to other modalities difficult. We propose to use Optical Coherence Tomography (OCT) to image the cortical architecture in the medial temporal lobe (MTL), at the entorhinal and perirhinal boundary (BA 28 and 35 respectively) and in the temporal isocortex. The acquisition is performed directly on the blockface to overcome registration issues. Perirhinal and entorhinal cortices have distinct cytoarchitecture and their boundaries have been delineated in *ex vivo* MRI model [4, 1]. Here, we build on this model to distinguish isocortical boundaries that are typically more subtle than mesocortical boundaries, and not easily visible with MRI.

## Methods and Materials

### Optical coherence tomography

OCT is an optical technique providing **3D high resolution** images up to several hundreds of microns in depth in biological tissue [5]. This technique avoids cutting, mounting or staining and greatly reduces deformations in the tissue. OCT detects differences in refractive index between tissues types, *e.g.* **cell bodies** and **myelinated fibers**.

**Our Set Up** [7]

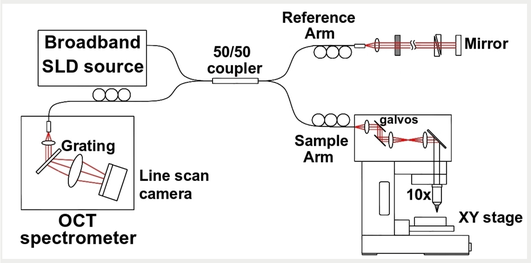


Axial resolution : 3.5 µm
Lateral resolution 3 µm
Field of View: 1.5x1.5 mm$^2$
Avg Int. Proj. (AIP) over 400 µm
Stitching

### Tissue Preparation

Temporal lobe samples were used for this study: two sample of MTL containing the entorhinal and perirhinal cortex boundary (BA 28 and 35 respectively) and five samples of isocortex (BA 36, 20, 21 and 22). The samples were fixed and sectioned to collect 50µm thick slices for histological staining. The blockface was photographed after each section. The slices were then hand mounted and stained with thionin. The remaining flat-faced tissue block was imaged with OCT.

### Qualitative comparison

Fig. 1 shows the blockface (A), Nissl stain (B) and OCT (C) images of one isocortical sample. Nissl and OCT have inversed contrast. The Nissl shows distortions due to histological protocol and tissue integrity, *e.g.* tissue rips, tissue overlaps or wide gaps between gyri (Fig. 1B, arrows). Distortions can impair registration to blockface image or to MRI data. OCT shows minimal if any distortions.

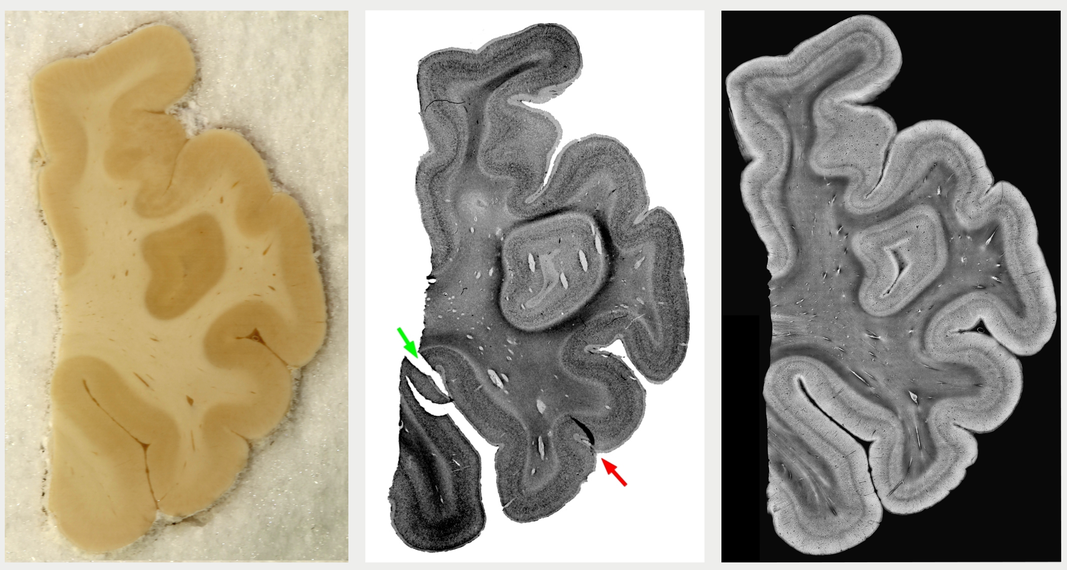

A B C

Fig. 1: A: Blockface, B: Nissl stain and C: OCT images of one of the isocortex samples.

## Entorhinal and Perirhinal cortex boundary [2]

Fig. 2A and 2B show the OCT images (AIP and maximum intensity projection MIP, respectively) where the boundary between entorhinal (EC) and perirhinal (PC) cortex is observed as well as perirhinal subdivisions, areas 35a and 35b. In OCT (Fig. 2A), neuron dense areas appear white, in contrast to the Nissl stained section (Fig. 2C). Neurons are particularly notable in layers II and IV in EC and layers II and III in PC (individual neurons visible on the MIP in Fig. 2B). The oblique layer routinely observed in area 35 showed dark signal.

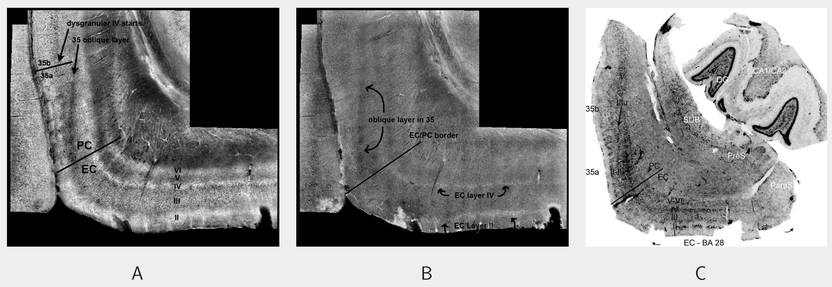


A B C

Fig. 2: A: AIP, B: MIP and C: Nissl stain of MTL sample at the border of EC and PC.

## Temporal Isocortex

The second experiment involves 5 isocortical samples (mean age 65.5, 2F/2M, 1 unknown). The most distiguishable architectonic features were manualy drawn on both Nissl and OCT images: the pial surface (PS), the gray/white matter boundary (GWB) and cortical layers (CL). Fig. 3A and 3B show the manual labeling on the Nissl and OCT images, respectively.

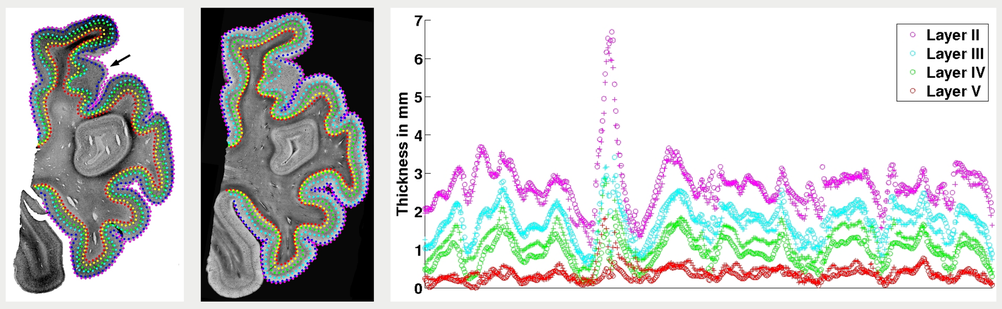


A B C

Fig. 3: Manual labeling of the cortical landmarks on co-registered Nissl stain (A) and OCT images (B). The drawn lines are the PS (magenta), the GWB (red) and the differents CL: layer II (dark blue), layer III (cyan), layer IV (green) and layer V (yellow). C: Thickness from GWB to CL.

The plot (Fig. 3C) shows the thickness between GWB and CL of the sample presented on Fig. 3A and 3B. The thicknesses are symbolized by + for the Nissl stains and by ○ for the OCT. Qualitatively, the thicknesses are in good accordance. The Pearson's correlation $\rho$ between the corresponding lines for both modalities was calculated for each sample, as well as their p-value. The mean Pearson's correlation was $\rho$=0.84 $\pm$ 0.16 with a very small p-value.

We have demonstrated that OCT labeling is as reliable as Nissl labeling. The labels drawn by two independent observers for each modality show no significant differences, evaluated by the Haussdorf distance and the median distance for each pair of lines (Fig. 4).

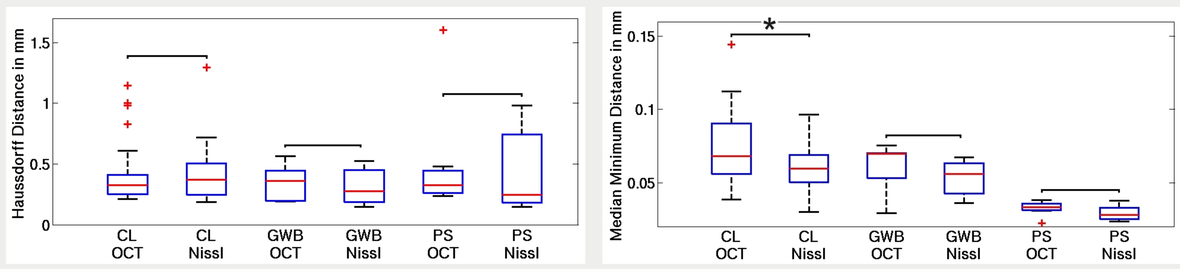


A B

Fig. 4: Statistical analysis for the inter-observer reliability. A: the Haussdorff distance, B: the median minimal distance. Wilcoxon signed rank test is shown above the bracket by $*$, if $\mathbf{p <= 0.05}$.

## Advantages of OCT

### ▶ Independent of tissue

The histological process and the *ex vivo* MRI are influenced by the tissue integrity and handling (aging, fixation, post mortem interval...) and/or affinity to dyes

### ▶ Registration to blockface and MRI

Fig. 5: Registration to blockface with Nissl (left) and OCT (right).

Histology protocol suffers from distortions (rips, deformations due to hand mounting or due to dehydration). Due to this, registration to the blockface images can be compromised (Fig. 5 left, arrow). Alternatively, OCT allows to image directly on the tissue block so that only minor distortions occur (Fig. 5, right).

### ▶ Cyto- and myelo- architectonic structures in cortical ribbon, as well as fibers in the white matter[1]

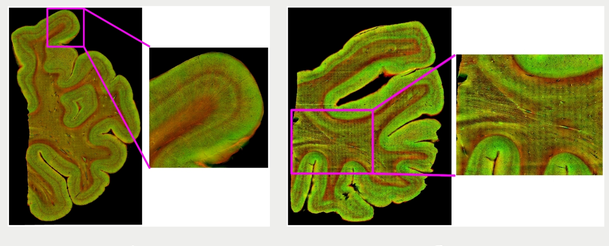

A B

Fig. 6: Overlay of MIP and AIP. A: Cyto- and myelo- architecture in the gray matter and B: connectivity in the white matter.

### ▶ 3D reconstruction

1. Using Optical Coherence Tomography to Validate Diffusion MRI, presented during O-Th2: Modeling and Analysis Methods 4: Multi-Modal and poster 3657

## Conclusions and Future Works

OCT is a promising tool for the localization of cortical boundaries. Indeed, in OCT data, especially the AIP, the laminar structure is similar to the one obtained by Nissl stain. However, contrary to histological staining, the tissue block is imaged, reducing considerably the deformations. Here 2D images were used to validate the technique but a future application will provide a 3D reconstruction of a volume of several cm$^3$ by adding a vibrotome to our setup [6]. The OCT cortical segmentation could be used as a training set for *in vivo* MRI boundary detection.

## References

[1] Jean C Augustinack, Kristen E Huber, Allison a Stevens, Michelle Roy, Matthew P Frosch, André J W van der Kouwe, Lawrence L Wald, Koen Van Leemput, Ann C McKee, and Bruce Fischl. Predicting the location of human perirhinal cortex, Brodmann's area 35, from MRI. *NeuroImage*, 64:32–42, August 2013.

[2] Jean C. Augustinack, Caroline Magnain, Martin Reuter, André J.W. van der Kouwe, David Boas, and Bruce Fischl. MRI Parcellation of Ex Vivo Medial Temporal Lobe. *NeuroImage*, in press, May 2013.

[3] Korbinian Brodmann. Vergleichende Lokalisationslehre der Grosshirnrinde in ihren Prinzipien dargestellt auf Grund des Zellenbaues. Verlag von Johann Ambrosius Barth, Leipzig (Germany), 1909.

[4] Bruce Fischl, Allison A Stevens, Niranjini Rajendran, B T Thomas Yeo, Douglas N Greve, Koen Van Leemput, Jonathan R Polimeni, Sita Kakunoori, Randy L Buckner, Jennifer Pacheco, David H Salat, Jennifer Melcher, Matthew P Frosch, Bradley T Hyman, P Ellen Grant, Bruce R Rosen, André J W van der Kouwe, Graham C Wiggins, Lawrence L Wald, and Jean C Augustinack. Predicting the location of entorhinal cortex from MRI. *NeuroImage*, 47(1):8–17, August 2009.

[5] David Huang, Eric A Swanson, Charles P Lin, Joel S Schuman, William G Stinson, Warren Chang, Michael R Hee, Thomas Flotte, Kenton Gregory, Carmen A Puliafito, and James G Fujimoto. Optical Coherence Tomography. *Science*, 254:1178–1181, 1991.

[6] Timothy Ragan, Jeremy D Sylvan, Ki Hean Kim, Hayden Huang, Karsten Bahlmann, Richard T Lee, and Peter T C So. High-resolution whole organ imaging using two-photon tissue cytometry. *J. Biomed. Opt.*, 12(1):014015, 2012.

[7] Vivek J Srinivasan, Harsha Radhakrishnan, James Y Jiang, Scott Barry, and Alex E Cable. Optical coherence microscopy for deep tissue imaging of the cerebral cortex with intrinsic contrast. *Opt. Express*, 20(3):2220–2239, January 2012.